

A 850 GHz Waveguide Receiver Employing a Niobium SIS Junction Fabricated on a $1\mu\text{m}$ Si_3N_4 Membrane

Jacob W. Kooi, Jérôme Pety, Bruce. Bumble, Christopher K. Walker, Henry G. LeDuc, P. L. Schaffer, and T.G. Phillips

Abstract— We report on a 850 GHz SIS heterodyne receiver employing a RF tuned niobium tunnel junction with a current density of $14\text{kA}/\text{cm}^2$, fabricated on a $1\mu\text{m}$ Si_3N_4 supporting membrane. Since the mixer is designed to be operated well above the superconducting gap frequency of niobium ($2\Delta/h \approx 690$ GHz), special care has been taken to minimize niobium transmission line losses. Both Fourier Transform Spectrometer measurements of the direct detection performance and calculations of the IF output noise with the mixer operating in heterodyne mode, indicate an absorption loss in the niobium film of about 6.8 dB at 822 GHz. These results are in reasonably good agreement with the loss predicted by the Mattis-Bardeen theory in the extreme anomalous limit. From 800–840 GHz we report uncorrected receiver noise temperatures of 518K or 514K when we use Callen & Welton's law to calculate the input load temperatures. Over the same frequency range, the mixer has a 4 dB conversion loss and $265\text{K} \pm 10\text{K}$ noise temperature. At 890 GHz the sensitivity of the receiver has degraded to 900K, which is primarily the result of increased niobium film loss in the RF matching network. When the mixer was cooled from 4.2K to 1.9K the receiver noise temperature improved about 20% to 409K DSB. Approximately half of the receiver noise temperature improvement can be attributed to a lower mixer conversion loss, while the remainder is due to a reduction in the niobium film absorption loss. At 982 GHz we measured a receiver noise temperature of 1916K.

Keywords— Niobium superconducting film absorption loss, silicon-nitride membrane, SIS tunnel junction.

I. INTRODUCTION

TO take advantage of the 780 to 950 GHz atmospheric window, for submillimeter astronomy, a full height waveguide superconducting-insulator-superconducting (SIS) heterodyne receiver with

Manuscript received December 13, 1996; revised November 21, 1997. This work was supported in part by grants from NASA (NAGW-107), and the NSF (AST93-13929). The junction fabrication was performed at the Center for Space Microelectronics Technology, Jet Propulsion Laboratory, California Institute of Technology, and was sponsored by NASA, Office of Space Access Technology.

J.W. Kooi, J. Pety, P.L. Schaffer, and T.G. Phillips are with the Downs Laboratory of Physics 320-47, California Institute of Technology, Pasadena, CA 91125, USA. E-mail: kooi@tacos.caltech.edu.

B. Bumble and H.G. LeDuc are with the Center for Space Microelectronics Technology, Jet Propulsion Laboratory 302-231, California Institute of Technology, Pasadena, CA 91109, USA.

C.K. Walker is with the Stewart Observatory at the University of Arizona, Tucson, AZ 85721, USA.

Publisher Item Identifier S 0018-9480(98)01591-9.

a center frequency of 850 GHz has been developed.

The results discussed here were achieved by using a $0.22\mu\text{m}^2$ Nb/ AlO_x /Nb tunnel junction fabricated on a $1\mu\text{m}$ Si_3N_4 membrane. The membrane is mounted on a pedestal which is centered over a full height rectangular waveguide. The mixer block is based on a design by Ellison *et al.* [1] and employs two circular non-contacting tuning elements [2], [3], magnetic field concentrators [7], and an integrated 1-2 GHz IF matching network [14].

Traditionally waveguide junctions have been constructed on quartz supporting substrates. To avoid RF leakage by means of surface modes down the quartz substrate, the cutoff frequency of these modes needs to be well above the operation frequency of the mixer. Unfortunately, the required thickness of the quartz and the dimensions of the substrate channel that hold the junction become unmanageably small for frequencies above 800 GHz. To avoid this problem we explored the idea of fabricating the junction on a $1\mu\text{m}$ Si_3N_4 membrane. At the frequencies of interest, the photons have energies larger than the superconducting energy gap of niobium, 2Δ , and are able to break Cooper pairs within the superconductor. This results in a large absorption loss in the niobium transmission line situated in front of the mixer, thereby seriously degrading the receiver sensitivity. From the superconducting transmission line theory [12], [16] we expect coupling efficiencies of about 30% with a $1/\sqrt{f}$ dependence. Detailed interpretation of the data confirm the $1/\sqrt{f}$ dependence, however the observed loss appears to be about one and a half times higher than the theoretically predicted loss. One possible explanation for the discrepancy is that based on the low current density in the niobium bowtie antenna and RF choke, we have assumed it's loss negligible compared to the loss in the RF matching network. The loss in the RF choke could however be significant since it is critically dependent on the way the membrane is mounted in the junction block. Independent from front-end loss calculations we derive, using the pumped and unpumped I/V curves, a 3.9–5 dB DSB mixer conversion loss from 800 GHz to 1 THz, thereby demonstrating that the SIS junction is still a highly efficient mixing element well above the superconducting gap. The receiver response is thus only significantly limited by the absorption loss in the RF matching network. To improve on the sensitivity of the receiver a better understanding of

higher Tc superconductor compound materials such as NbTiN or NbN and lower-loss wiring materials such as Al and Au [17] is needed.

II. JUNCTION DESIGN

Above the gap frequency of niobium, ($2\Delta/h \approx 690$ GHz), the photon energy is large enough to break Cooper-pairs in the superconductor, causing large absorption loss in the niobium film. To minimize the absorption loss (calculated to be 50-65% per wavelength at 850 GHz, depending on the SiO insulator thickness) in the RF tuning structure above the gap, it is important to keep the RF matching network as simple and short as possible. In Fig. 1 we compare the calculated coupling efficiencies of a radial stub and "end-loaded" stub RF matching network centered at 850 GHz [5], [6]. The "end-loaded" RF matching network typically employs two quarter-wave impedance transformer sections and a series inductive stub. The inductive stub is used to tune out the large junction susceptance, while the transformer provides a match to the much larger antenna impedance. Although the "end-loaded" stub matching network is successfully used with SIS devices below the gap frequency of niobium, above 700 GHz wiring loss prohibits it's use. For this reason we decided to use a radial stub RF matching network [9], [10]. It is interesting to note that this kind of matching network has a relative narrow bandwidth below the superconducting energy gap while above it the frequency response will be broadened due to the dispersive loss in the niobium film.

The radial stub matching network functions by effectively placing an inductance, made out of a small section of niobium transmission line, in parallel with the junction (Fig. 6). In doing so, it resonates out the large parasitic junction capacitance of the junction ($\omega R_n C \approx 8.6$ @ 850 GHz).

The loss in the niobium film (G_l) can be modeled as a conductance in parallel with the RF junction admittance, Y_{rf} , calculated from Tucker's theory [20]. For frequencies above that of the niobium gap Y_{rf} is typically slightly less than G_n , the junction normal state conductance. The embedding impedance seen by the junction, Y_{emb} in Fig. 7, thus includes a loss factor

$$G_p = \frac{G_l}{(1 + Q^2)}, \quad (1)$$

where G_l is the ohmic loss in the niobium film, Q the Quality factor of the lossy RF matching network, and G_p the equivalent parallel conductance. In our case, $Q^2 \gg 1$ and equation 1 simplifies to

$$G_p \simeq \frac{B_l^2}{G_l} \quad (2)$$

where B_l is the shunt susceptance of the inductive transmission line. Power coupled to the junction is maximized by employing small area devices which decrease the transmission line susceptance B_l . Secondly, the loss in the niobium can be decreased by maximizing the SiO insulating

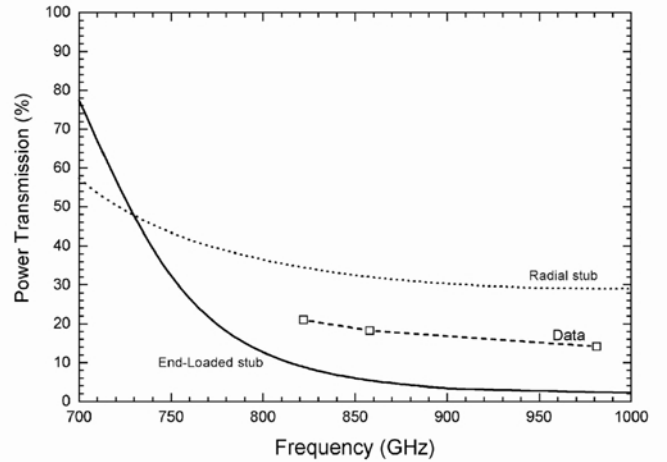


Fig. 1. Coupling efficiency calculations for both the Radial and "End-loaded" stub matching networks (solid curves), and calculated efficiency from the heterodyne data (dashed line). A 9.3% RF reflection loss is included, however the loss in the RF choke structure and Bowtie antenna are not included in the simulated result.

layer thickness to transmission line width ratio (G_l maximized). In our case we have opted for an insulator thickness of 450 nm, which is a standard process in the JPL-MDL junction fabrication process. Lastly, by employing high current density devices we increase Y_{rf} , by means of G_n , and thus increase the fraction of power coupled to the SIS device.

The properties of the superconducting microstrip lines are calculated using a method described by Zmuidzinas *et al.* [15]. The surface impedance is derived from the Mattis-Bardeen theory [16] in the extreme anomalous limit ($d \rightarrow \infty$ and $l \gg \delta$). Where d is the thickness of the niobium film, l the electron mean free path, and δ the penetration depth in niobium, ≈ 85 nm. Using a program written by Zmuidzinas & Bin we find that, given a 35 Ohm probe impedance (section III-B), optimum power transfer is obtained for a 70 Ohm junction with a current density of ≈ 10 kA/cm². The actual device described in this paper has a current density of 14.2 kA/cm², area of 0.22 μ m² and normal state resistance of 65 Ohm.

In section V-B we find that the embedding impedance seen by the junction at 822 GHz is about $25.4 + j0.63\Omega$. Knowing Z_{emb} , the junction capacitance and RF matching network parameters, we deduce an actual antenna impedance of $50.4 - j18\Omega$. Now using the actual, rather than the theoretical 35 Ω , antenna impedance in our computer model we calculate a reflection loss at the RF port of 9.3%. The calculated loss in Fig. 1 was derived by correcting the RF transmission t_{rf} (section V-B) for the front-end optics and RF matching network reflection losses.

III. RECEIVER CONFIGURATION

A. Mixer Block Construction

The front section of the mixer block is constructed on one mandrel in order to reduce the number of waveguide discontinuities and minimizes ohmic loss. It is composed of a cor-

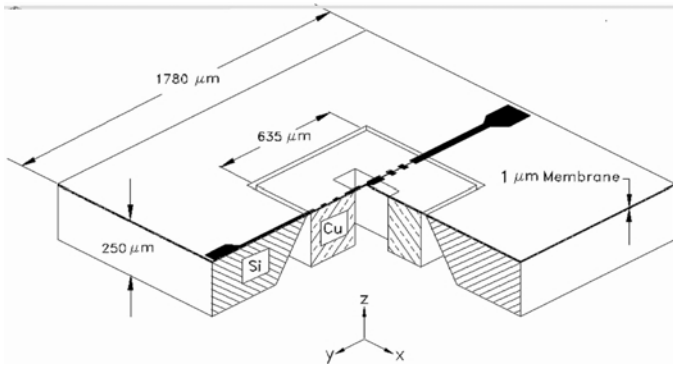


Fig. 2. Rendering of the $1\mu\text{m}$ Si_3N_4 membrane, RF choke and silicon support structure that houses the SIS tunnel junction and RF matching network.

rugated feedhorn, circular to rectangular waveguide transformer and E-plane tuner. The Si_3N_4 membrane structure and circular non-contacting backshort tuner make up the back section of the mixer-block. In our design, the E-plane tuner is situated $1/2 \lambda_g$ in front of the junction and incorporates magnetic field concentrators as discussed by Walker *et al.* [7].

To further optimize the performance of the receiver we have opted for the use of circular non-contacting E-plane and backshort tuners [2], [3]. These tuners consists of three beryllium copper concentric circular sections that extend from a rectangular shaft which is carefully fit in the waveguide. The low and high impedance sections have diameters of $100\mu\text{m}$ and $50\mu\text{m}$ respectively. Scale model measurements have indicated that the position of the tuner in the waveguide is not critical as long as wall contact by the round sections is avoided.

On the IF side, the junction is wire-bonded to the 1-2 GHz IF matching network [14], and the mixer block ground (Fig. 3). The matching network is designed to transform a 160 Ohm IF impedance to 50 Ohm and to provide a short to out of band signals up to ≈ 22 GHz to avoid saturating the junction with unwanted out of band signals. The output of the mixer block is directly connected to a cryogenic cooled 1-2 GHz balanced HEMT amplifier based on work by Padin *et al.* [8]. Reflections caused by the impedance mismatch between the matching network and low noise amplifier are partially absorbed by the amplifier's input Lange coupler ($S_{11} \leq -10$ dB).

B. Membrane Construction

Figure 2 depicts the Si_3N_4 membrane situated on top of a copper pedestal which houses the waveguide. The membrane itself is supported by silicon etched along the 111 crystal plane.

The membrane was placed on top of an optically polished flat copper pedestal which provides the ground plane for the microstrip mode RF choke (Fig. 3). A $100\mu\text{m}$ groove has been machined in the mixer horn block directly above the RF choke. The RF choke structure on top of the membrane provides a short circuit at the waveguide wall when the bowtie antenna and RF matching network are

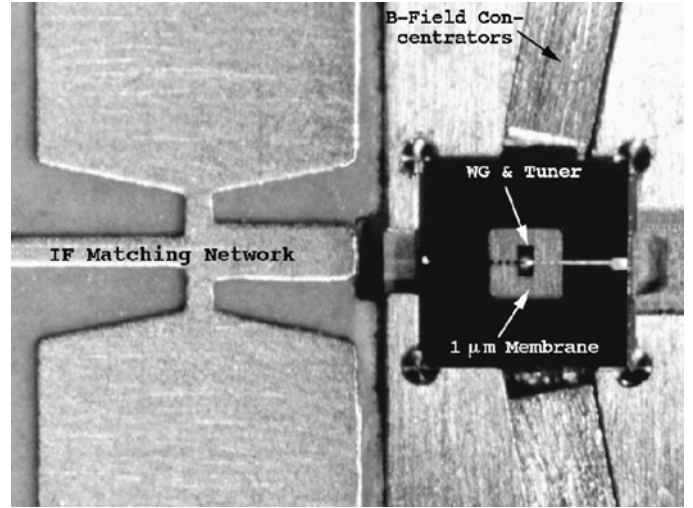


Fig. 3. View of the silicon nitride membrane situated in the mixer block. The membrane extends $50\mu\text{m}$ over the pedestal for stress relief. Looking through the membrane one sees the waveguide ($250 \times 125\mu\text{m}$) and outline of the circular tuner low impedance section ($100\mu\text{m}$ dia, about twice the size of a human hair).

centered in the waveguide.

Perhaps a better design incorporates a suspended RF stripline, which provides dimensional freedom in the Z-direction. A 2-3 μm PMMA spacer is placed between the junction block housing the membrane and the horn block to prevent the membrane from breaking when the two blocks are fit together in the final mixer assembly. The devices are glued into a "moat" by means of a 50% solution of nail polish (polyester resin) in butylacetate. Securing devices this way has the advantage that they are easily removed with acetone yet cycle securely to LHe temperatures. As far as we can tell, I/V characteristics of both LHe dipped junctions and those cooled in a vacuum dewar are identical. This is a good indication that the thermal conductivity of the silicon nitride membrane is high enough to prevent heating of the junction by infrared radiation.

To obtain a better understanding of the probe impedance of the bowtie antenna on top of the silicon nitride membrane mounted in the mixer block (see Fig. 3), we performed a series of scale model measurements. From it we determined an embedding impedance of about 35 Ohm, and have made the assumption in our computer simulations that this impedance is fixed (by adjusting both E-plane and backshort tuner accordingly).

C. Cooled Optics

The receiver noise temperature is critically dependent on t_{rf} , defined as the combined front-end optics and niobium film transmission coefficient,

$$T_{rec} = \frac{(T_{rf} + T_{mix} + T_{IF})}{t_{rf} G_{mix}^{DSB}}. \quad (3)$$

G_{mix}^{DSB} is the mixer gain and T_{rf} , T_{mix} , T_{IF} as the front-end, mixer and IF noise temperatures referred to the output of the mixer.

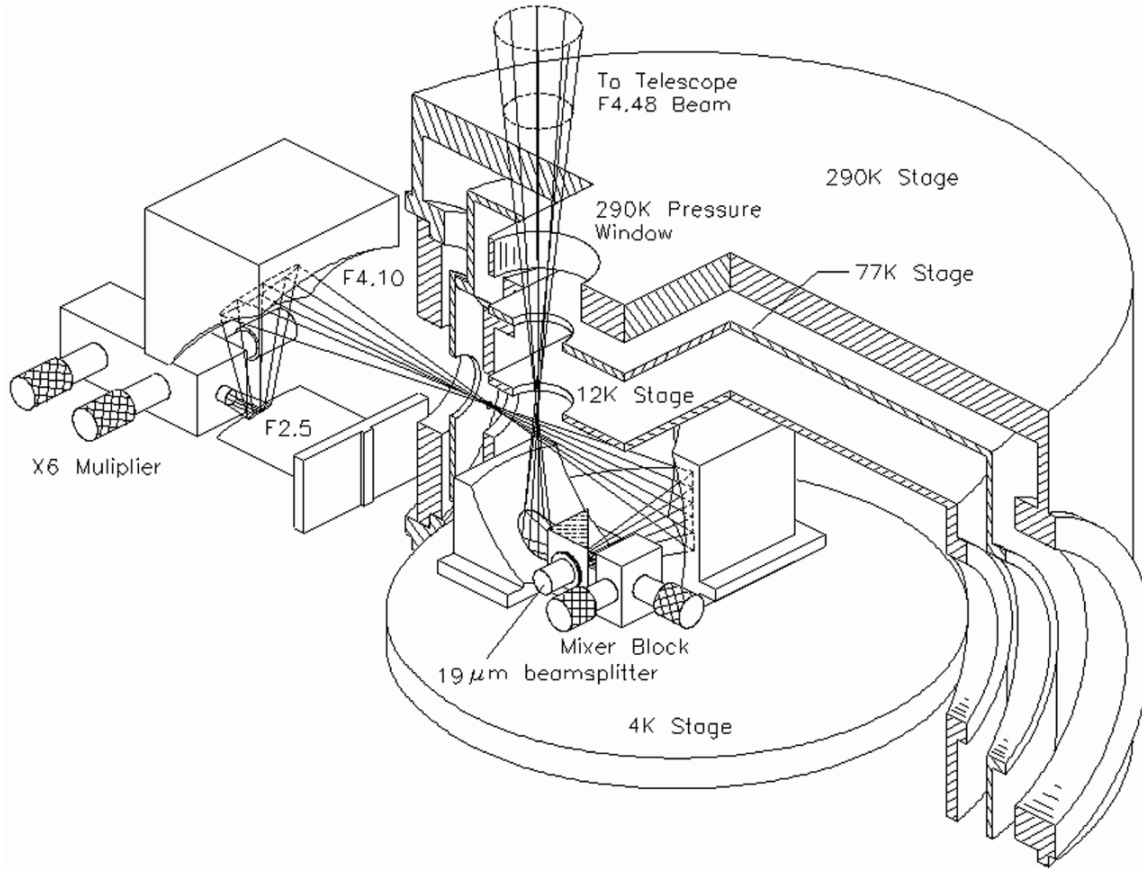


Fig. 4. Isometric cut-away view of the optics configuration employed. The cryostat is mounted up side down in the Cassegrain focus of Caltech Submillimeter Observatory (CSO).

From the point of view of optimizing the receiver performance we tried to maximize t_{rf} by carefully selecting the infrared blocking filters and eliminating the use of plastic lenses in the optics path. Furthermore to minimize the noise contribution from the 12% reflective mylar beamsplitter we decided to combine the RF and local oscillator power (LO) on the LHe stage. Figure 4 shows an isometric view of the optics configuration.

The corrugated feedhorn beamwidth was measured by Walker *et al.* on a scaled version at 115 GHz. It measures 10.5° at the ϵ^{-2} power contour in both E and H planes. This beam is transformed by means of an off-axis ellipsoidal mirror to an F4.48 beam with a 12 dB edge-taper at the secondary mirror of the telescope (Fig. 4). Both LO and RF beams have their second foci between the 12K and 77K stages of the cryostat. This allows the use of 40 mm diameter, 2.5 mm thick, crystal quartz pressure windows [36]. The IR blocks on the 77K stage are made out of 1.25 mm thick crystal quartz disks, 25 mm in diameter. The quartz lenses are anti-reflection coated with clear teflon ($n=1.44$) [34] [35]. At the 12K stage we use a 30–60% porous, 190 μ m thick, teflon sheet [37] to scatter the remaining infrared photons. Fourier transform spectrometer (FTS) transmission measurements of the teflon anti-reflection coated crystal quartz lenses indicate a 95–97% transmission efficiency in the submillimeter range. Hetero-

dine transmission measurements of the Zitex porous teflon material [37] at 822 GHz give 99% transmission per sheet, while spectrometer measurements in the near infrared (10 μ m) show a 98.5% loss per sheet, due to scattering of the IR photons.

Outside the dewar the local oscillator beam is re-focused, via a 45° flat mirror, to match the waist of the 780–870 GHz multiplier [13]. To help avoid standing waves between the secondary and the instrument, the vacuum windows and IR blocks were tilted at 5° angles. The receiver performance has been carefully measured with both the cooled beamsplitter/mirror and warm beamsplitter/cooled lens combination. All other hardware being the same, we noted an 75K reduction in receiver noise temperature when using the cooled beamsplitter/mirror configuration. Analyses of the data show that this is primarily due to the elimination of reflection loss of the 4K low density polyethelene lens, i.g. t_{rf} improved by about 8%.

To investigate the far-field beam (see Fig. 5) characteristics of the waveguide mixer, an antenna beam test stand was employed. The measurement technique involves using a lock-in amplifier to detect a chopped hot-load/cold-load signal source, while the source is moved normal to the E- and H- planes of the antenna beam. The hot load is a grooved piece of macor, attached to a heating element. The cold load is room-temperature Eccosorb. The signal

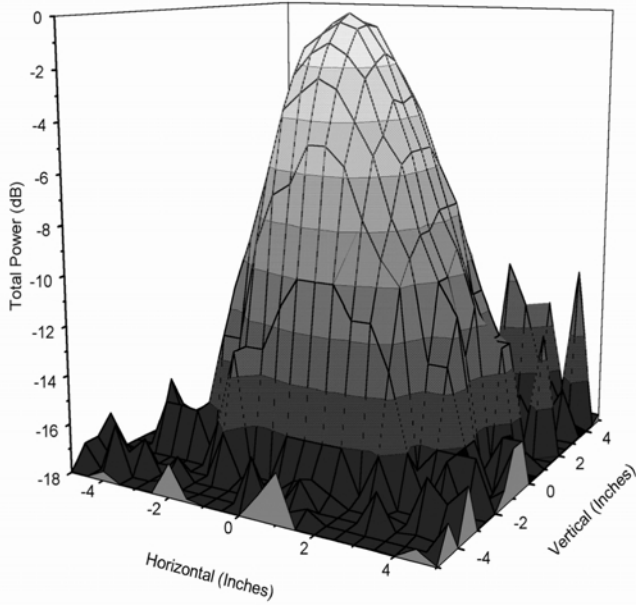


Fig. 5. Far field pattern of the receiver beam measured at 822 GHz. The beam matches the F4.48 telescope beam and has a 12 dB edge taper on the chopping secondary mirror.

source is aperture-limited, approximating a point source in the far-field.

IV. $\text{Nb}/\text{AlO}_x/\text{Nb}$ JUNCTION AND CHIP FABRICATION

Devices are fabricated on (100) oriented silicon wafers which are $254\mu\text{m}$ thick, 51mm diameter, and polished on both sides. The Si_3N_4 is grown under conditions for reduced stress by low pressure chemical vapor deposition (LPCVD) to a thickness of $1\mu\text{m}$. Fabrication of the $\text{Nb}/\text{AlO}_x/\text{Nb}$ tunnel junction is accomplished using a standard trilayer deposition technique [18], [19]. Magnetron sputter deposition and room temperature oxide growth are done in-situ in an ultra-high vacuum system with a base pressure of 2×10^{-9} Torr.

The trilayer is deposited by a lift-off process employing a multi-layer photolithographic technique using PMMA under AZ5214 photoresist. This step forms one side of the antenna/filter structure with layers of 160nm Nb base, 6nm Al, and 90nm Nb counter-electrode.

A junction mesa of $0.3\mu\text{m}^2$ area is defined by direct-write-electron beam lithography in a 100nm thick PMMA stencil. Chromium is deposited through the PMMA stencil and serves as an etch mask over 500nm of polyimide. Contact regions of the trilayer are then protected by adding a photoresist stencil. The combined chromium+photoresist/polyimide structure is etched using an oxygen reactive ion etch (RIE). Polyimide remaining defines an isolation window and junction mesa for subsequent Nb RIE. To achieve Nb etch directionality we utilize a gas mixture of $62\%\text{CCl}_2\text{F}_2 + 31\%\text{CF}_4 + 7\%\text{O}_2$. Electrical isolation of the base electrode from the wire layer is provided by thermal evaporation of 200nm of SiO. Samples

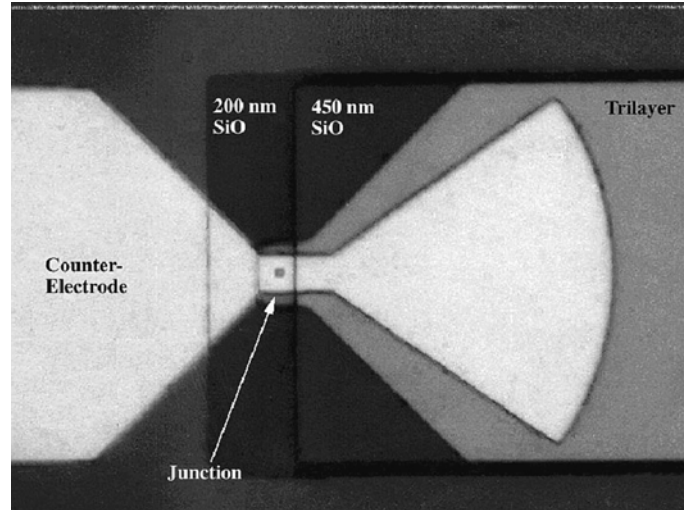


Fig. 6. 1000X photograph of the junction on silicon membrane. The transmission line length is $2.5\mu\text{m}$ on 450nm SiO which is terminated by a radial stub with a fan angle of 70 degrees. The junction size in the center of the bowtie antenna is $0.55\mu\text{m}$ on a side.

are rotated at a slight tilt angle during SiO deposition to assure both good isolation and self-aligned lift-off with the polyimide. Lift-off is done by dissolving the polyimide in dichloromethane. A subsequent photoresist pattern is used to produce a total SiO thickness of 450nm under the tuning stub element only. The second half of the antenna/filter is formed by a blanket deposition of 250nm Nb capped with 30nm gold for contacts. RIE etching with an AZ5206 photoresist stencil defines this final front side pattern. Window openings are patterned on the back side by infra-red alignment to the front. This step is masked with AZ5218 photoresist which enables $\text{CF}_4 + 19\%\text{O}_2$ RIE etching through the back side Si_3N_4 .

Exposed silicon areas on the back side are anisotropically etched in a bath of 30% KOH solution at 70°C . Etching stops after about eight hours when only the front side membrane and side (111) silicon planes are left exposed. The devices on the front are protected from the KOH solution by an "O"-ring enclosure. A layer of wax on the device side also helps localize wafer damage if one of the Si_3N_4 windows happens to break during KOH etching. Individual chips $1.78\text{mm} \times 1.78\text{mm}$ are diced from the wafer using a diamond saw.

Device yield with this process is typically lower than similar devices which we make on either Si or quartz substrates. We have not determined exactly how to increase yield, however many devices with current densities of about $12\text{ kA}/\text{cm}^2$ and subgap to normal state resistance ratios of greater than 10 have been fabricated on multiple wafer runs.

V. RECEIVER PERFORMANCE

A. FTS Measurements

To measure the response of the RF matching network we have tested junctions as direct detectors using a Fourier

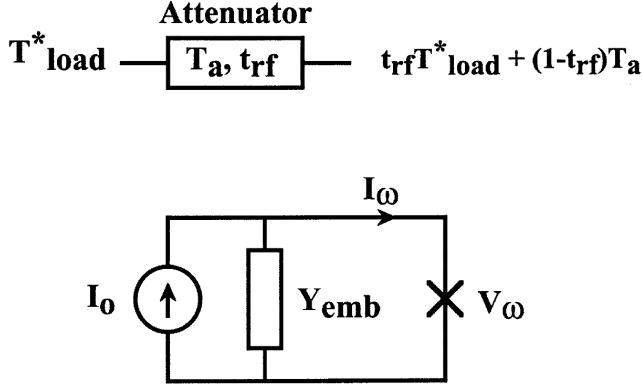


Fig. 7. RF port model used in our simulations.

Transform Spectrometer. The devices have been mounted quasi-optically against a quartz hyperhemispherical lens as described by Büttgenbach *et al.*[4]. The advantage of this method is that there are no external tuning elements in the system as in the case with a waveguide mount, and as such the overall frequency response of the junction can be measured.

The disadvantage is that the junction's bowtie antenna and RF choke are mounted slightly out of focus on the back of an hyper-hemispherical lens. This presents an unknown and frequency dependent embedding impedance, which affects the magnitude of the video response.

Compared to FTS measurements on 665 GHz tuned junctions the response of the 850 GHz tuned junctions on silicon nitride membrane has degraded ≈ 4 -7 dB. This is in fairly good agreement with the absorption loss predicted by the Mattis-Bardeen theory. Because of the many uncertainties in the optics of these quasi-optically mounted waveguide junctions and the quality of the junctions, it is not possible to quote a more precise number.

The measured response is shifted down in frequency, compared to design, by about 50 GHz, 6% [11].

B. SIS Simulations

To simulate the receiver response to a cold or hot load, we used a three port model as described by Tucker and Feldman *et al.*[20]. In our simulations all the harmonic sidebands are assumed to be shorted by the parasitic junction capacitance. Moreover, the receiver is assumed to work in a true double sideband mode, which means that the embedding admittance seen by the junction is identical at the USB, LSB and LO frequencies. This way the two RF ports can be described by a single circuit. To use this theory, we first find the RF and IF embedding admittance.

Figure 7 shows the RF port model which we divide into an attenuator stage and a lossless RF circuit. The attenuator takes into account the front-end optics loss and absorption loss in the niobium film of the tuning circuit. The lossless RF circuit is described as a current source I_0 whose admittance, Y_{emb} , is the embedding admittance seen by the junction.

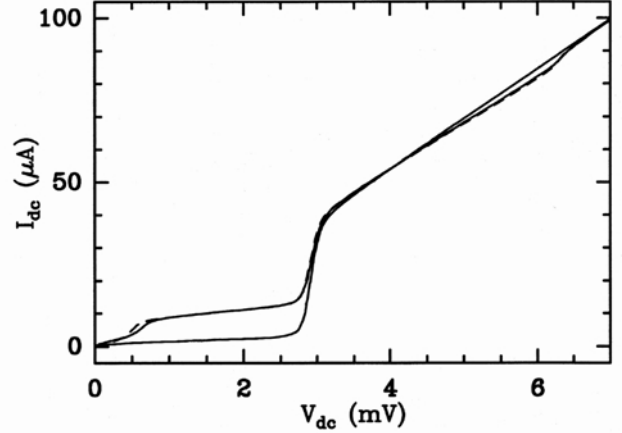


Fig. 8. Measured and calculated pumped and unpumped I/V curves. The optimum bias appears to be 2.25mV with a pumped LO current of 8.5 μ A which corresponds to $\alpha \equiv eV_w/\hbar\omega = 0.75$. The junction has a resistive subgap to R_n ratio of ≈ 10 .

The embedding admittance is deduced from a solution of the lossless RF circuit equation

$$I_{LO} = Y_{emb} \cdot V_w + I_w(V_{dc}, V_w), \quad (4)$$

where the RF junction current (I_w) is computed from the unpumped IV curve and its Kramers-Kronig transform (Equations (4.40) and (4.41) of Tucker & Feldman)[20]. Following Skalare[24], we first find the RF junction voltage ($V_w^k = \alpha^k \hbar\omega/e$) at each point k of the pumped IV curve (V_{dc}^k). With this set of points (all belonging to the first photon step), we are now able to find the parameters $|I_{LO}|$ and Y_{emb} which minimize the function

$$\sum_k \left| |I_{LO}|^2 - |Y_{emb} \cdot V_w^k + I_w(V_{dc}^k, V_w^k)|^2 \right|. \quad (5)$$

At 822 GHz we found $Z_{emb} = 25.4 + j0.63\Omega$ and $|I_{LO}| = 132.3\mu A$. Once Y_{emb} and $|I_{LO}|$ are known, we can compute the pumped IV curve (figure 8) and compare it with the measured data.

Figure 9 shows the IF port model. Here, the IF chain includes the matching network[14] and the IF amplifier. To characterize the IF noise contribution, Rudner & Feldman [21], and Woody, Miller & Wengler [22], proposed to use the unpumped junction above the gap voltage as a calibrated shot noise source. Two recent studies by Dubash *et al.*[25], [26] quantitatively verified that the noise current of an unpumped SIS junction is in fact the shot noise associated with the direct current. Using this study, Woody *et al.*[28] used the IF output power response of the unpumped mixer over the full I-V curve to completely characterize the IF chain.

To do so, they used the standard IF noise temperature[23] which is

$$T_{IFO} = T_{min} + T_d \frac{|Y_{opt} - Y_s|^2}{G_s G_{opt}} \quad (6)$$

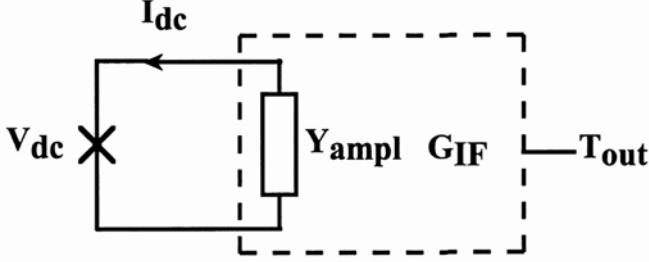


Fig. 9. IF port model

where $Y_s = G_s + jB_s$ is the input source admittance, T_{min} the minimum noise temperature, $Y_{opt} = G_{opt} + jB_{opt}$ the source admittance that achieves this minimum and T_d a measure of the noise sensitivity to deviations from Y_{opt} . This analysis allows a fit to the IF output power of the unpumped mixer using the model

$$P_{out} = g_{IF} G_{ampl} B \frac{2eI_{dc}^{unpumped} + 4kT_{IFO}G_s}{|Y_{ampl} + Y_s|^2}. \quad (7)$$

Here $Y_{ampl} = G_{ampl} + jB_{ampl}$ is the input admittance of the IF chain terminated by a 50 Ω load, g_{IF} the total IF gain, Y_s the IF output admittance of the junction and B the IF bandwidth. To fit to the measured IF output power, we have to rewrite the equation 7 as

$$P_{out} = g \frac{2eI_{dc} + aG_s^2 + bG_s + c + dB_s}{|Y_{ampl} + Y_s|^2} \quad (8)$$

where g, a, b, c, d , defined in Woody's paper, are combinations of $g_{IF}, B, T_{min}, T_d, Y_{opt}$ and Y_{ampl} .

Our experience is that the fitting procedure has two short-comings. First it can not distinguish between a large range of values for Y_{ampl} . To overcome this problem we fixed Z_{ampl} , well known from network measurements, to 160 Ω [14]. Secondly, for SIS heterodyne receivers, the mixer IF output susceptance is negligible (while the conductance is simply equal to the derivative of the IV curve). Because of this fact, the fitting procedure can not give the value of d , which prevents us from finding the exact values of T_{min}, T_d and Y_{opt} . We only are able to determine a range of values (See Table I). Knowing that a reasonable minimum IF noise temperature is $\approx 5K$, we obtain $T_d \approx 5.2K$, $R_{opt} \approx 145\Omega$ and $X_{opt} \approx -61\Omega$. While the actual physical values are difficult to find with precision, the fitting parameters are very well constrained by the data. This allows us to compute with good precision the IF noise contribution to the total output power as a function of the direct bias voltage for the pumped mixer. We only need to replace $I_{dc}^{unpumped}$ by I_{dc}^{pumped} in equation 8.

Using the Tucker theory [20] in the low IF approximation, we can then compute the DSB mixer gain, G_{mix}^{DSB} , and the noise power at the mixer output, T_{mix} , (Table II). The down converted quantum noise at the mixer output

 TABLE I
 RANGE OF ACCESSIBLE FITTING VALUES AT 822 GHz

| Parameter | Range |
|------------------------|-----------------|
| T_{min} (K) | 0.12 – 5.98 |
| T_d (K) | 2.74 – 5.66 |
| R_{opt} (Ω) | 76.69 – 155.5 |
| X_{opt} (Ω) | -137.1 – -22.89 |

 TABLE II
 MEASURED AND CALCULATED RECEIVER PARAMETERS AT 822 GHz
 FOR $V_{dc} = 2.25mV$ AND $\alpha = 0.75$.

| Parameters | Data* | Simulation* |
|-------------------------------------|--------|-------------|
| T_{rec} (K) | 514 | 514 |
| $T_a(1 - t_{rf})/t_{rf}$ (K) | 154 | 129 |
| T_{mix} (K) | 13.72 | 14.67 |
| T_{IF} (K) | 6.23 | 8.0 |
| G_{mix}^{DSB} (dB) | – | -4.0 |
| $t_{rf}G_{mix}^{DSB}$ (dB) | -12.57 | -12.3 |
| $T_{mix}/(t_{rf}G_{mix}^{DSB})$ (K) | 248 | 249 |
| $T_{IF}/(t_{rf}G_{mix}^{DSB})$ (K) | 112 | 136 |

is computed as explained by Wengler and Woody[27]. Finally, the RF attenuator (Fig. 7) is characterized by a transmission factor, t_{rf} , and a noise temperature T_a . t_{rf} and T_a can be found by adjusting the computed hot and cold total IF output power to fit the data. At 822 GHz, $t_{rf} = 0.146$ (-8.3 dB) and $T_a = 22.1K$. Given these values we compute an available LO power of 427 nW.

Figure 10 shows the total output power (bottom panel) as well as the decomposition in its different parts as a function of the bias voltage. All the simulated powers (in temperature units) are the powers dissipated in the IF matching network input admittance (Y_{ampl}). The mixer and IF noise temperatures T_{mix} and T_{IF} thus include the mismatch between the junction and the IF matching network. T_{IFO} used in equation 6 will be linked to T_{IF} by $T_{IF} = \Gamma_{IF}T_{IFO}$ where

$$\Gamma_{IF} = \frac{4G_sG_{11}}{|Y_{ampl} + Y_s|^2} = 0.83 \text{ at } 2.25 \text{ mV} \quad (9)$$

In figure 10 the dashed curves are the results for the cold load while the solid curves are the results for the hot load. Because the photon energy is larger than the gap frequency of niobium, the photon step overlap from the negative part of the IV curve (not shown here) partially cancels the photon step from the positive part of the IV curve. In the top panel we show the noise produced by the hot or cold loads at the input: $t_{rf}G_{mix}^{DSB}T_{load}^*$. In the text * indicates that the input load is defined using the Callen & Welton formula[31], [32] which gives for the hot and cold load 297.4K and 81.6K respectively. This is opposed to an uncorrected hot and cold load temperature of 297K and 80K in the Rayleigh-Jeans limit, as is common practice for lower frequency receivers. The emissivity of the cold load

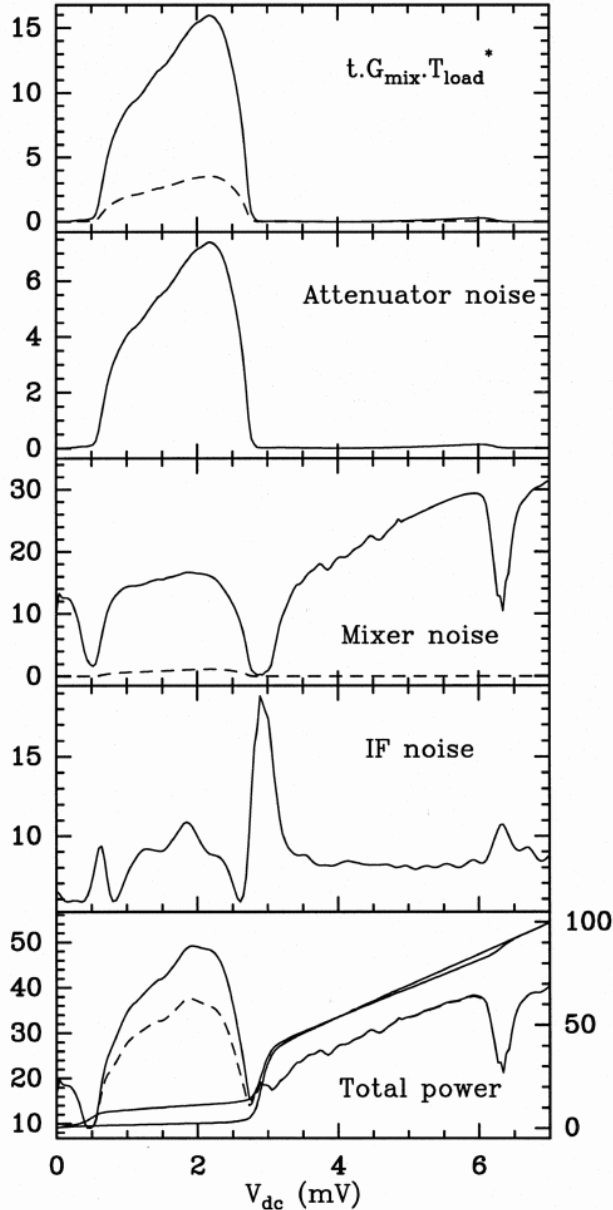


Fig. 10. Composition of the receiver output power at 822 GHz. Powers (left axis) are given in temperature units while the I/V curves (right axis) are in μA .

is estimated to be about 98%

The second panel from the top shows the attenuator noise contribution $G_{mix}^{DSB}(1 - t_{rf})T_a$. In the third panel we plot the mixer output noise power, which is made up of the shot noise in the mixer plus the quantum noise. The quantum noise which is the absolute receiver noise limit is shown as the dashed curve. The fourth curve is the IF noise contribution while the remaining curve is the total power, the sum of all the above curves.

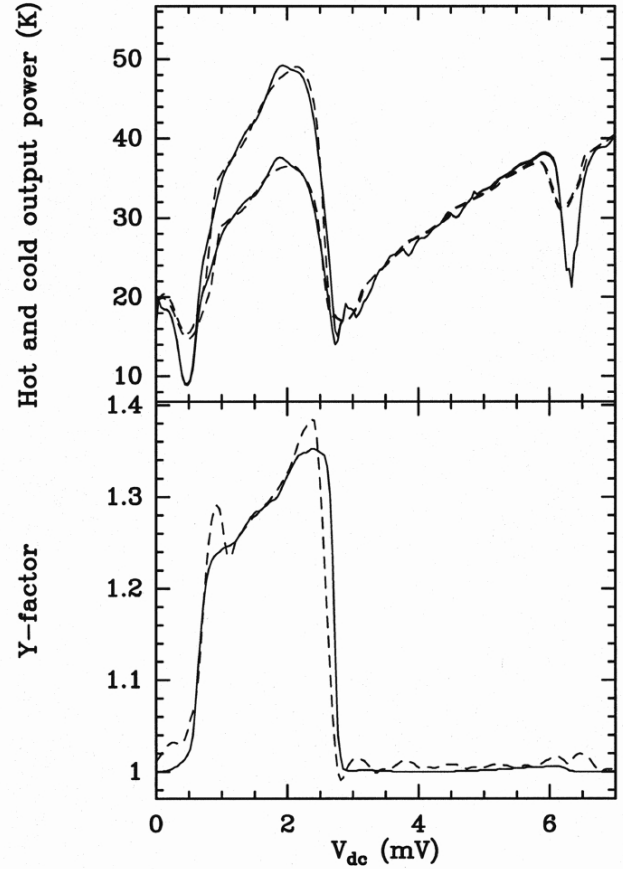


Fig. 11. Total power response at 822 GHz. The optimum receiver noise temperature at 822 GHz was $514 \pm 5\text{K DSB}$. At 1.9 Kelvin ambient temperature the corrected receiver noise temperature improved to 409K DSB . The solid curves are the data, while the dashed lines are the simulated results.

C. Heterodyne Results and Discussion

The 822 GHz measured and calculated hot and cold total power response is shown in Fig.11a. The Shapiro steps were carefully suppressed by adjusting the magnetic field. In Fig.11b. we show the measured and calculated Y factor (total power ratio). Note the good agreement between theory and measurement.

Table II tabulates the measured and simulated receiver parameters at 822 GHz. Using the intersecting line technique described by Blundell, Ke & Feldman *et al.* [29], [30] we derive a corrected front-end noise temperature of 154K^* . This compares to a simulated front-end noise temperature of 129K . Caution must be taken when directly comparing these results. The intersecting line technique is likely to include some small correction factors (τ) because the mixer is not perfectly matched and/or operating in true DSB mode [30]. The magnitude of τ is some fraction of $\hbar\omega/k = 39.5\text{K}$ at 822 GHz.

Using the Shot noise method [21], [22] we calculate an overall mixer conversion gain of -12.6 dB , mixer noise temperature of 248K and IF noise temperature (as referred to the output of the mixer) of 6.2K . These results are in good

TABLE III
MEASURED AND CALCULATED RECEIVER PARAMETERS FOR DIFFERENT FREQUENCIES AND AMBIENT TEMPERATURES.

| Parameters | 822 GHz at 1.9K | 858 GHz at 4.2K | 982 GHz at 4.2K |
|--|--------------------|--------------------|--------------------|
| T_{rec}^* (K) | 409 | 577 | 1916 |
| $T_a(1 - t_{rf})/t_{rf}$ (K) | 86 | 137 | 254 |
| T_{mix} (K) | 11.7 | 11.5 | 12.37 |
| T_{IF} (K) | 12.0 | 10.5 | 8.5 |
| $G_{\text{mix}}^{\text{DSB}}$ (dB) | -3.5 | -3.9 | -5.0 |
| $t_{rf}G_{\text{mix}}^{\text{DSB}}$ (dB) | -11.3 | -13.0 | -19.1 |
| $T_{\text{mix}}/(t_{rf}G_{\text{mix}}^{\text{DSB}})$ (K) | 159 | 230 | 1006 |
| $T_{IF}/(t_{rf}G_{\text{mix}}^{\text{DSB}})$ (K) | 164 | 210 | 656 |
| V_{gap} (mV) | 2.9 | 2.8 | 2.8 |

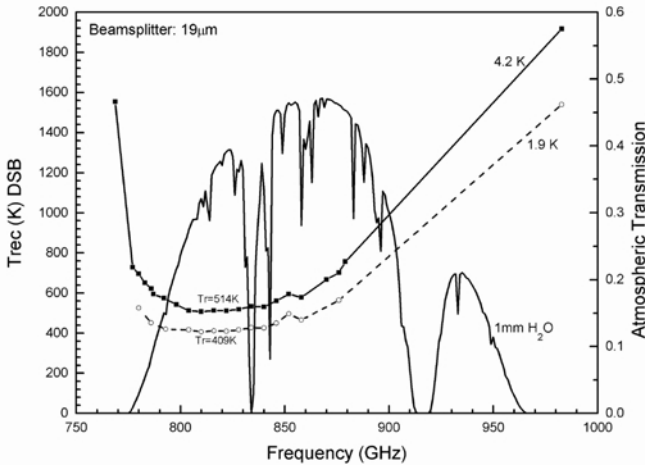


Fig. 12. Frequency response of the 850 GHz waveguide receiver discussed. The receiver employs an Radial stub RF matching network and two mechanical circular tuners. When installed at the Caltech Submillimeter Observatory(CSO) the receiver noise temperature improved 8% (475K @ 809 GHz) across the band which is attributed to the lower LHe bath temperature (3.55K) at the 4200 meter altitude site.

agreement with the simulation where we are able to separate the total front-end loss (8.3 dB) from the actual mixer down conversion loss (4 dB). From FTS measurements we estimate a total front-end optics loss of 1.1 dB and a RF mismatch of ≈ 0.42 dB (section II). This leaves a niobium absorption loss of about 6.8 dB (79%), due to the antenna, choke and RF matching network. The calculated loss compares favorably with earlier FTS measurements [11], and is about one and a half times the loss expected from the Mattis-Bardeen theory (65.4%).

When the mixer was cooled from 4.2K to 1.9K the receiver noise temperature improved about 20% to 409K DSB (Table III). Interpretation of the measurements show that $G_{\text{mix}}^{\text{DSB}}$ increases about 12% to -3.5 dB, which is similar to what is observed below the gap [3]. This can be attributed to the sharpening of the I/V curve. An additional 12.2% improvement in the front-end transmission, t_{rf} is gained as the result of a slightly higher energy gap ($\approx 2.9\text{mV}$), and

therefore reduced loss in the niobium film.

At 858 GHz we calculate a DSB mixer down conversion loss and front-end loss of 3.9 and 9.1 dB respectively. Of the 9.1 dB about 1.2 dB is due to loss in the optics while another ≈ 0.5 dB is caused by reflection loss of the RF matching network. The calculated niobium film transmission loss at 858 GHz is therefore $\approx 82\%$, as opposed to a theoretically expected loss of 68%.

At 982 GHz the DSB mixer conversion gain has degraded to about -5 dB, which comes as no surprise since we are tuned away from the resonant peak. The front-end reflection loss at this frequency is about 1.8 dB, so that we have a niobium transmission loss of 87% (8.8 dB), assuming in this case a RF reflection loss of 0.5 dB.

From this discussion it is clear that the niobium SIS junction is still a highly efficient mixing element up to at least 1 THz (2.9Δ) [33] but that the loss in the niobium film is severely limiting the receiver sensitivity (Fig. 1). Given the performance of the mixer, receiver noise temperatures as low as 250-300K DSB at 1 THz should be achievable with a higher T_c ($\geq 14\text{K}$) superconducting materials such as NbTiN.

The measured frequency response of the 850 GHz receiver at both 4.2 and 1.9 Kelvin is shown in figure 12. At 982 GHz the sensitivity has degraded to 1916K, DSB, which is primarily due to the loss in the niobium tuning circuit. In all circumstances the receiver was tuned for maximum IF power, which occurs when $G_{\text{mix}}^{\text{DSB}}$ is optimized.

VI. OBSERVATIONS

In December 1996 we observed ^{12}CO $J = 7 \rightarrow 6$ (807 GHz) and detected atomic carbon, $\text{CI } 2 \rightarrow 1$ (809 GHz) in the Orion Bar region, at the Caltech Submillimeter Observatory. System temperature and total integration time were $\sim 4400\text{K}$ and 47 minutes respectively. The main beam efficiency measured on Mars ($10''$ diameter) was 33%, while the approximate zenith atmospheric transmissions was 40%. The spectrum was corrected for an estimated extended source coupling efficiency of 60%

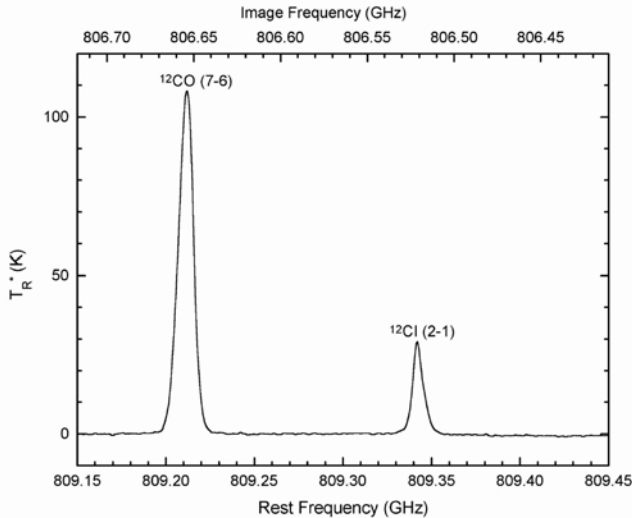


Fig. 13. A spectrum of the Orion Bar in ^{12}CO $J = 7 \rightarrow 6$ and $\text{Cl} \rightarrow 1$, taken at the Caltech Submillimeter Observatory.

VII. CONCLUSION

We have discussed the design and development of a 850 GHz waveguide heterodyne receiver employing a tuned $0.22\mu\text{m}^2$ Nb/ AlO_x /Nb SIS tunnel junction on a $1\mu\text{m}$ silicon nitride membrane. The membrane is mounted on a copper pedestal with the bowtie antenna centered on the waveguide. To take advantage of the accuracy that can be achieved with silicon micromachining, it is recommended that for future THz applications a micromachined waveguide mount and suspended stripline membrane design be combined.

We have demonstrated the effectiveness of the radial stub RF matching network to tune out the large parasitic junction capacitance and minimize the absorption loss of the niobium film above the superconducting energy gap of niobium.

Direct detection response measurements with a Fourier Transform Spectrometer indicate response from 700–1100 GHz which are confirmed by Josephson resonances in the I-V curve. Calculations of the niobium absorption loss on the measured heterodyne data confirms the expected $1/\sqrt{f}$ dependence. Both heterodyne and direct detection response measurements give a loss and a half times higher than predicted by the Mattis-Bardeen theory. Although the origin of the excess loss is not completely clear, it is important to note the generally good agreement with the theory.

From 800–840 GHz we report corrected receiver noise temperatures of 514K DSB in the laboratory and 475K DSB at the Observatory due to the lower LHe bath temperature at the high elevation. Over the same frequency range we calculate a DSB mixer conversion gain of about -4 dB, a mixer noise of $\approx 265\text{K}$, and a front-end loss of $\approx 130\text{K}$. At 890 GHz the sensitivity has degraded to 900K, which is primarily a result of the increased loss in the niobium film. Cooling the mixer to 1.9K, the receiver noise temperature from 790–840 GHz improved about 20% due

to a slightly higher and sharper niobium energy gap. The receiver response is clearly limited by the absorption loss in the RF matching network, and to improve the sensitivity of the receiver a better understanding of higher T_c superconductor compound materials such as NbTiN or NbN and lower-loss wiring materials such as Al and Au is needed.

VIII. ACKNOWLEDGEMENTS

We wish to thank Prof. Jonas Zmuidzinis, Mei Bin, Rob Schoelkopf, Benson Chan, John Ward, Todd Hunter, Tony Kerr, and Mark Feldman for helpful discussions, Ken Young (Taco), Jocelyn Keene and Darek Lis for help with the observations, Professor Yu-Chong Tai and his group at Caltech for the silicon nitride deposition, Dave Miller for help with the optics measurements, Dave Tahmoush and Dominic Benford for help with the IR transmission and reflection measurements, Keith Horvath for his superb craftsmanship on making the mixer block, Rüdiger Zimmerman (RPG-Radiometer) for his excellent and hard work on the 780–870 and 982 GHz multipliers, John Carlstrom for his enduring work on the 130-146 GHz Gunn oscillator, Bob Weber and Walt Schaal for their work on the 3-D modeling, Martin Gould for his incredible over night machining abilities, and lastly Kooi thanks his wife for her faithful support.

REFERENCES

- [1] B.N. Ellison and R.E. Miller, "A Low Noise 230 GHz SIS Receiver," *Int. J. IR and MM Waves*, vol. 8, 609-625, 1987
- [2] A. R. Kerr, "An Adjustable Short-Circuit for Millimeter Waveguides," *Electronics Division Internal Report No. 280*, National Radio Astronomy Observatory, Charlottesville, VA 22903, July 1988.
- [3] J.W. Kooi, C.K. Walker, H.G. LeDuc, T.R. Hunter, D.J. Benford, and T.G. Phillips, "A Low Noise 665 GHz SIS Quasi-Particle Waveguide Receiver," *Int. J. IR and MM Waves*, vol. 15, No. 3, 477-492, 1994.
- [4] T.H. Büttgenbach, H.G. LeDuc, P.D. Maker, T.G. Phillips "A fixed tuned broadband matching structure for submillimeter receivers," *IEEE Trans. Applied Supercond.*, vol. 2, No. 3, pp. 165-175, September 1992.
- [5] J. W. Kooi, M. Chan, B. Bumble, and T. G. Phillips, "A low noise 345 GHz waveguide receiver employing a tuned $0.50\mu\text{m}^2$ Nb/ AlO_x /Nb tunnel junction," *Int. J. IR and MM Waves*, vol. 15, No. 5, May 1994.
- [6] J. W. Kooi, M. Chan, B. Bumble, H. G. Leduc, P.L. Schaffer, and T. G. Phillips "230 and 492 GHz Low-Noise SIS Waveguide Receivers employing tuned Nb/ AlO_x /Nb tunnel junctions," *Int. J. IR and MM Waves*, vol. 16, No. 12, pp. 2049-2068, Dec. 1995
- [7] C. K. Walker, J. W. Kooi, M. Chan, H. G. Leduc, P.L. Schaffer, J.E. Carlstrom, and T.G. Phillips, "A Low-noise 492 GHz SIS waveguide receiver," *Int. J. IR and MM Waves*, vol. 13, pp. 785-798, June 1992.
- [8] S. Padin, G. Ortiz. "A Cooled 1-2 GHz Balanced HEMT Amplifier," *IEEE Trans. Microwave Theory and Techniques*, vol 39, No 7, pp 1239-1243, 1991.
- [9] M. Salez, P. Febre, W.R. McGrath, B. Bumble, H.G. LeDuc, "An SIS Waveguide Heterodyne Receiver for 600 GHz- 635GHz," *Intl. J. IR and MM Waves*, vol. 15, No.2, 349-368, Feb. 1994.
- [10] P. Febre, W.R. McGrath, P. Batelaan, B. Bumble, H.G. LeDuc, S. George, P. Featrier, "A Low-Noise SIS Receiver Measured from 480 GHz to 650 GHz using Nb Junctions with Integrated RF Tuning Circuits," *Intl. J. IR and MM Waves*, vol. 15, No.6, June 1994.
- [11] J.W. Kooi, M.S. Chan, M. Bin, B. Bumble, H.G. Leduc, C.K. Walker, and T.G. Phillips, "The Development of an 850 GHz Waveguide Receiver using Tuned SIS Junctions on $1\mu\text{m}$ Si_3N_4 Membranes," *Int. J. IR and MM Waves*, V16 (2), pp 349-362, Feb. 1995

- [12] R. Pöpel, "Electromagnetic Properties of Superconductors," pp. 44-78 in V. Kose, ed., *Superconducting Quantum Electronics*, Springer-Verlag: Berlin, 1989.
- [13] R. Zimmerman, T. Rose, T.W. Crowe, T.W. Grein, "An All-Solid-State 1 THz Radiometer For Space Applications", *6th Int. Symp. on Space THz Technology*, Caltech, Ca, March 1995.
- [14] J.W. Kooi, M. Chan, T.G. Phillips, B. Bumble, and H.G. LeDuc, "A low noise 230 GHz heterodyne receiver employing $0.25\ \mu\text{m}^2$ area Nb/ AlO_x /Nb tunnel junctions," *IEEE trans. Microwaves Theory and Techniques*, vol. 40, pp. 812-815, May 1992.
- [15] J. Zmuidzinas and H.G. LeDuc, "Quasi-optical slot antenna SIS mixers," *IEEE trans. Microwaves Theory and Techniques*, vol. 40, No. 9, pp. 1797-1804, Sept. 1992.
- [16] D.C. Mattis and J. Bardeen, "Theory of the anomalous skin effect in normal and superconducting metals," *Phys. Rev.*, vol 111, pp. 412-417, 1958
- [17] M.Bin, M.C. Gaidis, J. Zmuidzinas, T.G. Phillips, and H.G. LeDuc, "THz SIS Mixers with Normal Metal Al Tuning Circuits," submitted to *Supercond. Sci. Tech.*, October, 1995.
- [18] M.Gurivch, M.A. Washington, and H.A. Huggins, "High quality refractory Josephson tunnel Junction utilizing thin aluminum layers", *Appl. Phys. Lett.*, vol. 42, 472-474, 1983.
- [19] H.G. LeDuc, B. Bumble, S.R. Cypher and J.A. Stern, *Second International Symposium on Space Terahertz Technology*, Pasadena, CA, Feb. 26-28 (1991).
- [20] J.R. Tucker, and M.J. Feldman "Quantum Detection at Millimeter Wavelengths", *Rev. Mod. Phys.*, vol. 57, pp. 1055-1113, October 1985.
- [21] S. Rudner, M.J. Feldman, E. Kollberg, and T. Claeson, "Superconducting-Insulator-Superconducting Mixing with Arrays at Millimeter-Wave Frequencies", *J. Applied Physics*, vol. 52, pp. 6366-ff, 1981.
- [22] D.P. Woody, R.E. Miller, and M.J. Wengler, "85-115 GHz Receivers for Radio Astronomy", *IEEE Trans. Microwave Theory Tech.*, vol. 33, pp. 90-95, February 1985.
- [23] J. Lange, "Noise Characterization of Linear Two Ports in Terms of Invariant Parameters", *IEEE J. Solid State Circuits*, vol. SC-2, pp. 37-40, June 1967.
- [24] A. Skalare, "Determining Embedding Circuit Parameters from DC Measurements on Quasiparticles Mixers", *Int. J. IR and MM Waves*, vol. 10, pp. 1339-1353, 1989.
- [25] N.B. Dubash, G Pance, and M.J. Wengler, "Photon Noise in the SIS detector", *Fourth International Symposium on Terahertz technology*, UCLA, 1993.
- [26] N.B. Dubash, M.J. Wengler, and J. Zmuidzinas, "Shot Noise and Photon-Induced Correlations in 500 GHz SIS Detectors", *IEEE Trans. Applied Superconductivity*, vol. 5, no. 2, pp. 3308-3311, June 1995.
- [27] M.J. Wengler, and D.P. Woody, "Quantum Noise in Heterodyne Detection", *IEEE J. Quantum Electronics*, vol. 23, pp. 613-622, 1987.
- [28] D.P. Woody, S. Padin, H. LeDuc, and J. Stern, "On Using the Shot Noise in SIS Tunnel Junctions for Characterizing IF Amplifiers", *Sixth International Symposium on Space Terahertz Technology*, Caltech, March 21-23, 1995
- [29] R.Blundell, R.E. Miller, and K.H. Gundlach, "Understanding Noise in SIS Receivers," *Int. J. IR and MM Waves*, vol. 13, No. 1, pp. 3-26, 1992.
- [30] Q. Ke, and M.J. Feldman, "A Technique for Noise Measurements of SIS Receivers", *IEEE Trans. Microwave Theory Tech.*, vol. 42, No. 4 pp. 752-755, April 1994.
- [31] H.B. Callen and T.A. Welton, "Irreversibility and generalized Noise," *Phys. Rev.*, Vol. 83, no. 1, pp. 34-40, July 1951.
- [32] A.R. Kerr, M.J. Feldman, S.K. Pan, "Receiver Noise Temperature, the Quantum Noise Limit, and the Role of the Zero-Point Fluctuations." *NRAO Electronics Division Internal Report*, No. 304, Sept 1996.
- [33] D. Winkler and T. Claeson, "High Frequency Limits of Superconducting Tunnel Junction Mixers," *J. Appl. Phys.*, vol. 62, pp. 4482-4498, 1987.
- [34] Thermech Engineering Corp., 1773 W. Lincoln Ave., Bldg. K, Anaheim, CA 92801.
- [35] Francis Lord Optics, 33 Higginbotham Road, Gladesville, NSW 2111, Australia
- [36] Valpey-Fisher, A Subsidiary of Matec, 75 South Street, Hopkinton, MA 01748
- [37] Norton performance Plastics, 150 Dey Road, Wayne, NJ 07470

Jacob W. Kooi was born in Geldrop, The Netherlands on July 12, 1960. He received his B.S. degree in Microwave Engineering at the California Polytechnic State University in San Luis Obispo, California in 1985 and a M.S. degree in Electrical Engineering from the California Institute of Technology in 1992. His research interests are in the area of Millimeter and Submillimeter Wave technology and their applications.

Jérôme Pety was born in Lille, France on June 27, 1970. He received his B.S. degree in Physics at the Ecole Normale Supérieure, Paris, France, in 1993. He is currently doing his Ph.D. work at the Ecole Normale Supérieure. His research interests are in the area of superconducting devices and their application to submillimeter astronomy.

Bruce Bumble is a Member of Technical Staff at the Jet Propulsion Laboratory. He received a BE in Engineering Physics from Stevens Institute of Technology in 1982 and a MS in Materials Science from Polytechnic University of New York in 1989. His activities since then have been in the field of superconducting device fabrication for radio astronomy applications. He has been a member of the American Vacuum Society for 14 years and participated in the Applied Superconductivity Conferences

since 1986.

Christopher K. Walker was born in Shelby, N.C. on December 20, 1957. He received his B.S. in electrical engineering from Clemson University in 1980 and an M.S. in electrical engineering from Ohio State University in 1981. He then worked as a microwave engineer at TRW Areospace in Redondo Beach, CA and the Jet Propulsion Laboratory in Pasadena, CA from 1981 to 1983. In 1983, he became a graduate student in astronomy at the University of Arizona, where he received a Ph.D.

in 1988. His thesis research was on protostellar evolution and radio astronomy instrumentation. Upon graduation, he was awarded a Millikan Fellowship in Physics at Caltech. At Caltech he continued his work in protostellar evolution and then returned to the University of Arizona as an Assistant Professor of Astronomy. He is now an Associate Professor of Astronomy at the University of Arizona.

Henry G. LeDuc was born in Butte, MT on March 8, 1955. He received a B.S. in physics from Montana State University, Bozeman, MT in 1977, and a Ph.D. in physics from the University of California, Davis in 1983. His thesis work involved far-infrared spectroscopy of solid state ionic conductors. At present, he is a group leader at the California Institute of Technology's Jet Propulsion Laboratory. His group develops SIS tunnel junctions for heterodyne receivers.